BABAR-PUB-13/004
SLAC-PUB-15424

Measurement of the $D^*(2010)^+$ meson width and the $D^*(2010)^+ - D^0$ mass difference

J. P. Lees,[1] V. Poireau,[1] V. Tisserand,[1] E. Grauges,[2] A. Palano[ab],[3] G. Eigen,[4] B. Stugu,[4] D. N. Brown,[5] L. T. Kerth,[5] Yu. G. Kolomensky,[5] M. J. Lee,[5] G. Lynch,[5] H. Koch,[6] T. Schroeder,[6] C. Hearty,[7] T. S. Mattison,[7] J. A. McKenna,[7] R. Y. So,[7] A. Khan,[8] V. E. Blinov[ac],[9] A. R. Buzykaev[a],[9] V. P. Druzhinin[ab],[9] V. B. Golubev[ab],[9] E. A. Kravchenko[ab],[9] A. P. Onuchin[ac],[9] S. I. Serednyakov[ab],[9] Yu. I. Skovpen[ab],[9] E. P. Solodov[ab],[9] K. Yu. Todyshev[ab],[9] A. N. Yushkov[a],[9] D. Kirkby,[10] A. J. Lankford,[10] M. Mandelkern,[10] B. Dey,[11] J. W. Gary,[11] O. Long,[11] G. M. Vitug,[11] C. Campagnari,[12] M. Franco Sevilla,[12] T. M. Hong,[12] D. Kovalskyi,[12] J. D. Richman,[12] C. A. West,[12] A. M. Eisner,[13] W. S. Lockman,[13] A. J. Martinez,[13] B. A. Schumm,[13] A. Seiden,[13] D. S. Chao,[14] C. H. Cheng,[14] B. Echenard,[14] K. T. Flood,[14] D. G. Hitlin,[14] P. Ongmongkolkul,[14] F. C. Porter,[14] R. Andreassen,[15] C. Fabby,[15] Z. Huard,[15] B. T. Meadows,[15] M. D. Sokoloff,[15] L. Sun,[15] P. C. Bloom,[16] W. T. Ford,[16] A. Gaz,[16] U. Nauenberg,[16] J. G. Smith,[16] S. R. Wagner,[16] R. Ayad,[17,*] W. H. Toki,[17] B. Spaan,[18] K. R. Schubert,[19] R. Schwierz,[19] D. Bernard,[20] M. Verderi,[20] S. Playfer,[21] D. Bettoni[a],[22] C. Bozzi[a],[22] R. Calabrese[ab],[22] G. Cibinetto[ab],[22] E. Fioravanti[ab],[22] I. Garzia[ab],[22] E. Luppi[ab],[22] L. Piemontese[a],[22] V. Santoro[a],[22] R. Baldini-Ferroli,[23] A. Calcaterra,[23] R. de Sangro,[23] G. Finocchiaro,[23] S. Martellotti,[23] P. Patteri,[23] I. M. Peruzzi,[23,†] M. Piccolo,[23] M. Rama,[23] A. Zallo,[23] R. Contri[ab],[24] E. Guido[ab],[24] M. Lo Vetere[ab],[24] M. R. Monge[ab],[24] S. Passaggio[a],[24] C. Patrignani[ab],[24] E. Robutti[a],[24] B. Bhuyan,[25] V. Prasad,[25] M. Morii,[26] A. Adametz,[27] U. Uwer,[27] H. M. Lacker,[28] P. D. Dauncey,[29] U. Mallik,[30] C. Chen,[31] J. Cochran,[31] W. T. Meyer,[31] S. Prell,[31] A. E. Rubin,[31] A. V. Gritsan,[32] N. Arnaud,[33] M. Davier,[33] D. Derkach,[33] G. Grosdidier,[33] F. Le Diberder,[33] A. M. Lutz,[33] B. Malaescu,[33] P. Roudeau,[33] A. Stocchi,[33] G. Wormser,[33] D. J. Lange,[34] D. M. Wright,[34] J. P. Coleman,[35] J. R. Fry,[35] E. Gabathuler,[35] D. E. Hutchcroft,[35] D. J. Payne,[35] C. Touramanis,[35] A. J. Bevan,[36] F. Di Lodovico,[36] R. Sacco,[36] G. Cowan,[37] J. Bougher,[38] D. N. Brown,[38] C. L. Davis,[38] A. G. Denig,[39] M. Fritsch,[39] W. Gradl,[39] K. Griessinger,[39] A. Hafner,[39] E. Prencipe,[39] R. J. Barlow,[40,‡] G. D. Lafferty,[40] E. Behn,[41] R. Cenci,[41] B. Hamilton,[41] A. Jawahery,[41] D. A. Roberts,[41] R. Cowan,[42] D. Dujmic,[42] G. Sciolla,[42] R. Cheaib,[43] P. M. Patel,[43,§] S. H. Robertson,[43] P. Biassoni[ab],[44] N. Neri[a],[44] F. Palombo[ab],[44] L. Cremaldi,[45] R. Godang,[45,¶] P. Sonnek,[45] D. J. Summers,[45] X. Nguyen,[46] M. Simard,[46] P. Taras,[46] G. De Nardo[ab],[47] D. Monorchio[ab],[47] G. Onorato[ab],[47] C. Sciacca[ab],[47] M. Martinelli,[48] G. Raven,[48] C. P. Jessop,[49] J. M. LoSecco,[49] K. Honscheid,[50] R. Kass,[50] J. Brau,[51] R. Frey,[51] N. B. Sinev,[51] D. Strom,[51] E. Torrence,[51] E. Feltresi[ab],[52] M. Margoni[ab],[52] M. Morandin[a],[52] M. Posocco[a],[52] M. Rotondo[a],[52] G. Simi[a],[52] F. Simonetto[ab],[52] R. Stroili[ab],[52] S. Akar,[53] E. Ben-Haim,[53] M. Bomben,[53] G. R. Bonneaud,[53] H. Briand,[53] G. Calderini,[53] J. Chauveau,[53] Ph. Leruste,[53] G. Marchiori,[53] J. Ocariz,[53] S. Sitt,[53] M. Biasini[ab],[54] E. Manoni[a],[54] S. Pacetti[ab],[54] A. Rossi[a],[54] C. Angelini[ab],[55] G. Batignani[ab],[55] S. Bettarini[ab],[55] M. Carpinelli[ab],[55,**] G. Casarosa[ab],[55] A. Cervelli[ab],[55] F. Forti[ab],[55] M. A. Giorgi[ab],[55] A. Lusiani[ac],[55] B. Oberhof[ab],[55] E. Paoloni[ab],[55] A. Perez[a],[55] G. Rizzo[ab],[55] J. J. Walsh[a],[55] D. Lopes Pegna,[56] J. Olsen,[56] A. J. S. Smith,[56] R. Faccini[ab],[57] F. Ferrarotto[a],[57] F. Ferroni[ab],[57] M. Gaspero[ab],[57] L. Li Gioi[a],[57] G. Piredda[a],[57] C. Bünger,[58] O. Grünberg,[58] T. Hartmann,[58] T. Leddig,[58] C. Voß,[58] R. Waldi,[58] T. Adye,[59] E. O. Olaiya,[59] F. F. Wilson,[59] S. Emery,[60] G. Hamel de Monchenault,[60] G. Vasseur,[60] Ch. Yèche,[60] F. Anulli[a],[61] D. Aston,[61] D. J. Bard,[61] J. F. Benitez,[61] C. Cartaro,[61] M. R. Convery,[61] J. Dorfan,[61] G. P. Dubois-Felsmann,[61] W. Dunwoodie,[61] M. Ebert,[61] R. C. Field,[61] B. G. Fulsom,[61] A. M. Gabareen,[61] M. T. Graham,[61] C. Hast,[61] W. R. Innes,[61] P. Kim,[61] M. L. Kocian,[61] D. W. G. S. Leith,[61] P. Lewis,[61] D. Lindemann,[61] B. Lindquist,[61] S. Luitz,[61] V. Luth,[61] H. L. Lynch,[61] D. B. MacFarlane,[61] D. R. Muller,[61] H. Neal,[61] S. Nelson,[61] M. Perl,[61] T. Pulliam,[61] B. N. Ratcliff,[61] A. Roodman,[61] A. A. Salnikov,[61] R. H. Schindler,[61] A. Snyder,[61] D. Su,[61] M. K. Sullivan,[61] J. Va'vra,[61] A. P. Wagner,[61] W. F. Wang,[61] W. J. Wisniewski,[61] M. Wittgen,[61] D. H. Wright,[61] H. W. Wulsin,[61] V. Ziegler,[61] W. Park,[62] M. V. Purohit,[62] R. M. White,[62,††] J. R. Wilson,[62] A. Randle-Conde,[63] S. J. Sekula,[63] M. Bellis,[64] P. R. Burchat,[64] T. S. Miyashita,[64] E. M. T. Puccio,[64] M. S. Alam,[65] J. A. Ernst,[65] R. Gorodeisky,[66] N. Guttman,[66] D. R. Peimer,[66] A. Soffer,[66] S. M. Spanier,[67] J. L. Ritchie,[68] A. M. Ruland,[68] R. F. Schwitters,[68] B. C. Wray,[68] J. M. Izen,[69] X. C. Lou,[69] F. Bianchi[ab],[70] F. De Mori[ab],[70] A. Filippi[a],[70] D. Gamba[ab],[70] S. Zambito[ab],[70]

L. Lanceri[ab],[71] L. Vitale[ab],[71] F. Martinez-Vidal,[72] A. Oyanguren,[72] P. Villanueva-Perez,[72] H. Ahmed,[73] J. Albert,[73] Sw. Banerjee,[73] F. U. Bernlochner,[73] H. H. F. Choi,[73] G. J. King,[73] R. Kowalewski,[73] M. J. Lewczuk,[73] T. Lueck,[73] I. M. Nugent,[73] J. M. Roney,[73] R. J. Sobie,[73] N. Tasneem,[73] T. J. Gershon,[74] P. F. Harrison,[74] T. E. Latham,[74] H. R. Band,[75] S. Dasu,[75] Y. Pan,[75] R. Prepost,[75] and S. L. Wu[75]

(The *BABAR* Collaboration)

[1]*Laboratoire d'Annecy-le-Vieux de Physique des Particules (LAPP), Université de Savoie, CNRS/IN2P3, F-74941 Annecy-Le-Vieux, France*

[2]*Universitat de Barcelona, Facultat de Fisica, Departament ECM, E-08028 Barcelona, Spain*

[3]*INFN Sezione di Bari[a]; Dipartimento di Fisica, Università di Bari[b], I-70126 Bari, Italy*

[4]*University of Bergen, Institute of Physics, N-5007 Bergen, Norway*

[5]*Lawrence Berkeley National Laboratory and University of California, Berkeley, California 94720, USA*

[6]*Ruhr Universität Bochum, Institut für Experimentalphysik 1, D-44780 Bochum, Germany*

[7]*University of British Columbia, Vancouver, British Columbia, Canada V6T 1Z1*

[8]*Brunel University, Uxbridge, Middlesex UB8 3PH, United Kingdom*

[9]*Budker Institute of Nuclear Physics SB RAS, Novosibirsk 630090[a], Novosibirsk State University, Novosibirsk 630090[b], Novosibirsk State Technical University, Novosibirsk 630092[c], Russia*

[10]*University of California at Irvine, Irvine, California 92697, USA*

[11]*University of California at Riverside, Riverside, California 92521, USA*

[12]*University of California at Santa Barbara, Santa Barbara, California 93106, USA*

[13]*University of California at Santa Cruz, Institute for Particle Physics, Santa Cruz, California 95064, USA*

[14]*California Institute of Technology, Pasadena, California 91125, USA*

[15]*University of Cincinnati, Cincinnati, Ohio 45221, USA*

[16]*University of Colorado, Boulder, Colorado 80309, USA*

[17]*Colorado State University, Fort Collins, Colorado 80523, USA*

[18]*Technische Universität Dortmund, Fakultät Physik, D-44221 Dortmund, Germany*

[19]*Technische Universität Dresden, Institut für Kern- und Teilchenphysik, D-01062 Dresden, Germany*

[20]*Laboratoire Leprince-Ringuet, Ecole Polytechnique, CNRS/IN2P3, F-91128 Palaiseau, France*

[21]*University of Edinburgh, Edinburgh EH9 3JZ, United Kingdom*

[22]*INFN Sezione di Ferrara[a]; Dipartimento di Fisica e Scienze della Terra, Università di Ferrara[b], I-44122 Ferrara, Italy*

[23]*INFN Laboratori Nazionali di Frascati, I-00044 Frascati, Italy*

[24]*INFN Sezione di Genova[a]; Dipartimento di Fisica, Università di Genova[b], I-16146 Genova, Italy*

[25]*Indian Institute of Technology Guwahati, Guwahati, Assam, 781 039, India*

[26]*Harvard University, Cambridge, Massachusetts 02138, USA*

[27]*Universität Heidelberg, Physikalisches Institut, D-69120 Heidelberg, Germany*

[28]*Humboldt-Universität zu Berlin, Institut für Physik, D-12489 Berlin, Germany*

[29]*Imperial College London, London, SW7 2AZ, United Kingdom*

[30]*University of Iowa, Iowa City, Iowa 52242, USA*

[31]*Iowa State University, Ames, Iowa 50011-3160, USA*

[32]*Johns Hopkins University, Baltimore, Maryland 21218, USA*

[33]*Laboratoire de l'Accélérateur Linéaire, IN2P3/CNRS et Université Paris-Sud 11, Centre Scientifique d'Orsay, F-91898 Orsay Cedex, France*

[34]*Lawrence Livermore National Laboratory, Livermore, California 94550, USA*

[35]*University of Liverpool, Liverpool L69 7ZE, United Kingdom*

[36]*Queen Mary, University of London, London, E1 4NS, United Kingdom*

[37]*University of London, Royal Holloway and Bedford New College, Egham, Surrey TW20 0EX, United Kingdom*

[38]*University of Louisville, Louisville, Kentucky 40292, USA*

[39]*Johannes Gutenberg-Universität Mainz, Institut für Kernphysik, D-55099 Mainz, Germany*

[40]*University of Manchester, Manchester M13 9PL, United Kingdom*

[41]*University of Maryland, College Park, Maryland 20742, USA*

[42]*Massachusetts Institute of Technology, Laboratory for Nuclear Science, Cambridge, Massachusetts 02139, USA*

[43]*McGill University, Montréal, Québec, Canada H3A 2T8*

[44]*INFN Sezione di Milano[a]; Dipartimento di Fisica, Università di Milano[b], I-20133 Milano, Italy*

[45]*University of Mississippi, University, Mississippi 38677, USA*

[46]*Université de Montréal, Physique des Particules, Montréal, Québec, Canada H3C 3J7*

[47]*INFN Sezione di Napoli[a]; Dipartimento di Scienze Fisiche, Università di Napoli Federico II[b], I-80126 Napoli, Italy*

[48]*NIKHEF, National Institute for Nuclear Physics and High Energy Physics, NL-1009 DB Amsterdam, The Netherlands*

[49]*University of Notre Dame, Notre Dame, Indiana 46556, USA*

[50]*Ohio State University, Columbus, Ohio 43210, USA*

[51]*University of Oregon, Eugene, Oregon 97403, USA*

[52]*INFN Sezione di Padova[a]; Dipartimento di Fisica, Università di Padova[b], I-35131 Padova, Italy*

[53] Laboratoire de Physique Nucléaire et de Hautes Energies,
IN2P3/CNRS, Université Pierre et Marie Curie-Paris6,
Université Denis Diderot-Paris7, F-75252 Paris, France
[54] INFN Sezione di Perugia[a]; Dipartimento di Fisica, Università di Perugia[b], I-06123 Perugia, Italy
[55] INFN Sezione di Pisa[a]; Dipartimento di Fisica,
Università di Pisa[b]; Scuola Normale Superiore di Pisa[c], I-56127 Pisa, Italy
[56] Princeton University, Princeton, New Jersey 08544, USA
[57] INFN Sezione di Roma[a]; Dipartimento di Fisica,
Università di Roma La Sapienza[b], I-00185 Roma, Italy
[58] Universität Rostock, D-18051 Rostock, Germany
[59] Rutherford Appleton Laboratory, Chilton, Didcot, Oxon, OX11 0QX, United Kingdom
[60] CEA, Irfu, SPP, Centre de Saclay, F-91191 Gif-sur-Yvette, France
[61] SLAC National Accelerator Laboratory, Stanford, California 94309 USA
[62] University of South Carolina, Columbia, South Carolina 29208, USA
[63] Southern Methodist University, Dallas, Texas 75275, USA
[64] Stanford University, Stanford, California 94305-4060, USA
[65] State University of New York, Albany, New York 12222, USA
[66] Tel Aviv University, School of Physics and Astronomy, Tel Aviv, 69978, Israel
[67] University of Tennessee, Knoxville, Tennessee 37996, USA
[68] University of Texas at Austin, Austin, Texas 78712, USA
[69] University of Texas at Dallas, Richardson, Texas 75083, USA
[70] INFN Sezione di Torino[a]; Dipartimento di Fisica Sperimentale, Università di Torino[b], I-10125 Torino, Italy
[71] INFN Sezione di Trieste[a]; Dipartimento di Fisica, Università di Trieste[b], I-34127 Trieste, Italy
[72] IFIC, Universitat de Valencia-CSIC, E-46071 Valencia, Spain
[73] University of Victoria, Victoria, British Columbia, Canada V8W 3P6
[74] Department of Physics, University of Warwick, Coventry CV4 7AL, United Kingdom
[75] University of Wisconsin, Madison, Wisconsin 53706, USA

Measurements of the mass difference Δm_0 between the $D^*(2010)^+$ and the D^0 mesons and of the natural line width Γ of the transition $D^*(2010)^+ \to D^0\pi^+$ are presented. The data were recorded with the *BABAR* detector at center-of-mass energies at and near the $\Upsilon(4S)$ resonance, and correspond to an integrated luminosity of approximately $477\,\mathrm{fb}^{-1}$. The D^0 meson is reconstructed in the decay modes $D^0 \to K^-\pi^+$ and $D^0 \to K^-\pi^+\pi^-\pi^+$. For the decay mode $D^0 \to K^-\pi^+$ we obtain $\Gamma = (83.4 \pm 1.7 \pm 1.5)$ keV and $\Delta m_0 = (145\,425.6 \pm 0.6 \pm 1.8)$ keV, where the quoted uncertainties are statistical and systematic, respectively. For the $D^0 \to K^-\pi^+\pi^-\pi^+$ mode we obtain $\Gamma = (83.2 \pm 1.5 \pm 2.6)$ keV and $\Delta m_0 = (145\,426.6 \pm 0.5 \pm 2.0)$ keV. The combined measurements yield $\Gamma = (83.3 \pm 1.3 \pm 1.4)$ keV and $\Delta m_0 = (145\,425.8 \pm 0.5 \pm 1.8)$ keV; the result for the width is approximately 12 times more precise than the current world average, while that for the mass difference is more precise by a factor of approximately 6.

PACS numbers: 13.20.Fc, 13.25Ft, 14.40.Lb, 12.38.Gc, 12.38.Qk, 12.39.Ki, 12.39.Pn

The line width of the $D^*(2010)^+$ (D^{*+}) provides a window into a nonperturbative regime of strong interaction physics where the charm quark is the heavier meson constituent [1–3]. The line width provides an experimental test of D meson spectroscopic models, and is related to the strong coupling of the $D^*D\pi$ system, $g_{D^*D\pi}$. In the heavy-quark limit, which is not necessarily a good approximation for the charm quark [4], this coupling can be related to the universal coupling of heavy mesons to a pion, $\hat{g}$. Since the decay $B^* \to B\pi$ is kinematically forbidden, it is not possible to measure the coupling $g_{B^*B\pi}$ directly. However, the D and B systems can be related through $\hat{g}$, allowing the calculation of $g_{B^*B\pi}$, which is needed for a model-independent extraction of $|V_{ub}|$ [5, 6] and which forms one of the larger theoretical uncertainties for the determination of $|V_{ub}|$ [7].

We study the $D^{*+} \to D^0\pi^+$ transition, using the $D^0 \to K^-\pi^+$ and $D^0 \to K^-\pi^+\pi^-\pi^+$ decay modes, to extract values of the D^{*+} width Γ and the difference between the D^{*+} and D^0 masses Δm_0. Values are reported in natural units and the use of charge conjugate reactions is implied throughout this paper. The most precise prior measurement of the width [8], by the CLEO Collaboration, is $\Gamma = (96 \pm 4 \pm 22)$ keV, where the uncertainties are statistical and systematic, respectively. In the present analysis, we use a data sample that is approximately 50 times larger. This allows us to apply restrictive selection criteria to reduce background and to investigate sources of systematic uncertainty with high precision.

To extract Γ, we fit the distribution of the mass difference between the reconstructed D^{*+} and the D^0 masses, Δm. The signal component is described with a P-wave relativistic Breit-Wigner (RBW) function convolved with a resolution function based on a Geant4 Monte Carlo (MC) simulation of the detector response [9]. The detector resolution (full-width at half-maximum) for Δm is approximately 300 keV, which is larger than the measured value of Γ [8]. The key to this analysis is that, while

the full-width at half-maximum of the almost-Gaussian resolution is larger than the extracted width, the RBW tails allow us to use information far from the central signal region to measure the width. Consequently, we pay particular attention to how the selection criteria affect the tails.

This analysis is based on a data set corresponding to an integrated luminosity of approximately 477 fb^{-1} recorded at, and 40 MeV below, the $\Upsilon(4S)$ resonance. The data were collected with the *BABAR* detector at the PEP-II asymmetric energy e^+e^- collider, located at the SLAC National Accelerator Laboratory. The *BABAR* detector is described in detail elsewhere [10]; we summarize the relevant features below. The momenta of charged particles are measured with a combination of a cylindrical drift chamber (DCH) and a 5-layer silicon vertex tracker (SVT), both operating within the 1.5 T magnetic field of a superconducting solenoid. Information from a ring-imaging Cherenkov detector is combined with specific ionization (dE/dx) measurements from the SVT and DCH to identify charged kaon and pion candidates. Electrons are identified, and photons measured, with a CsI(Tl) electromagnetic calorimeter. The return yoke of the superconducting coil is instrumented with tracking chambers for the identification of muons.

We remove a large amount of combinatorial and B meson decay background by requiring D^{*+} mesons produced in $e^+e^- \to c\bar{c}$ reactions to exhibit an e^+e^- center-of-mass-frame momentum greater than 3.6 GeV. The entire decay chain is fit using a kinematic fitter with geometric constraints at the production and decay vertex of the D^0 and the additional constraint that the D^{*+} laboratory momentum point back to the interaction region of the event. The pion from D^{*+} decay is referred to as the "slow pion" (denoted π_s^+) because of the limited phase space available in the D^{*+} decay. The selection criteria are chosen to provide a large signal-to-background ratio (S/B), in order to increase the sensitivity to the long signal (RBW) tails in the Δm distribution; they are not optimized for statistical significance. The criteria are briefly mentioned here and presented in detail in the archival reference for this analysis [11]. The experimental uncertainty in Δm is dominated by the uncertainty on the measured momentum of the slow pion. We implement criteria to select well-measured pions. We define our acceptance angle to exclude the very-forward region of the detector, where track momenta are not accurately reconstructed, as determined using an independent sample of reconstructed $K_S^0 \to \pi^-\pi^+$ decays. The K_S^0 reconstructed mass is observed to vary as a function of the polar angle θ of the K_S^0 momentum measured in the laboratory frame with respect to the electron beam axis. To remove contributions from the very-forward region of the detector we reject events with any D^{*+} daughter track for which $\cos\theta > 0.89$; this reduces the final samples by approximately 10%.

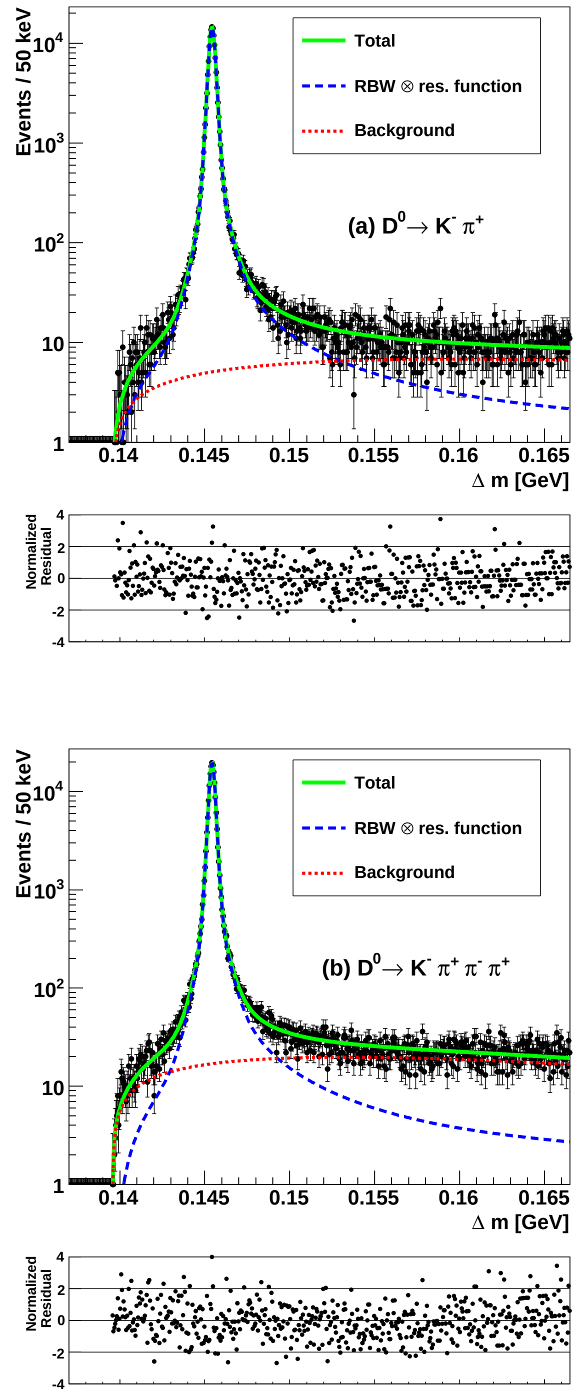

FIG. 1. (color online) Fits to data for the $D^0 \to K^-\pi^+$ and $D^0 \to K^-\pi^+\pi^-\pi^+$ decay modes. The total probability density function (PDF) is shown as the solid curve, the convolved RBW-Gaussian signal as the dashed curve, and the background as the dotted curve. The total PDF and signal component are indistinguishable in the peak region. Normalized residuals are defined as $(N_{\text{observed}} - N_{\text{predicted}})/\sqrt{N_{\text{predicted}}}$.

Our fitting procedure involves two steps. In the first step we use the sum of three Gaussians and a threshold-like function [11] to model the finite detector resolution associated with track reconstruction, by fitting the Δm distribution for correctly reconstructed MC events. These simulated D^{*+} decays are generated with $\Gamma = 0.1\,\mathrm{keV}$, so that the observed spread of the MC distribution can be attributed to event reconstruction. The threshold function describes π_s^+ decays in flight to a μ, for which coordinates from both the π and μ segments are used in track reconstruction.

The second step uses the resolution shape parameters from the first step and convolves the Gaussian components with a RBW function to fit the measured Δm distribution in data. The RBW function is defined by

$$\frac{d\Gamma(m)}{dm} = \frac{m\Gamma_{D^*D\pi}(m)\; m_0\Gamma}{\left(m_0^2 - m^2\right)^2 + \left(m_0\Gamma_{\mathrm{Total}}(m)\right)^2}, \qquad (1)$$

where $\Gamma_{D^*D\pi}$ is the partial width to $D^0\pi_s^+$, m is the $D^0\pi_s^+$ invariant mass, m_0 is the invariant mass at the pole, and $\Gamma_{\mathrm{Total}}(m)$ is the total D^{*+} decay width. The partial width is defined by

$$\Gamma_{D^*D\pi}(m) = \Gamma\left(\frac{\mathcal{F}^{\ell}_{D\pi}(p_0)}{\mathcal{F}^{\ell}_{D\pi}(p)}\right)^2 \left(\frac{p}{p_0}\right)^{2\ell+1} \left(\frac{m_0}{m}\right). \qquad (2)$$

Here $\ell = 1$, $\mathcal{F}^{\ell=1}_{D\pi}(p) = \sqrt{1 + r^2p^2}$ is a Blatt-Weisskopf form factor for a vector particle with radius parameter r and daughter momentum p, and the subscript zero denotes a quantity measured at the mass pole m_0 [12, 13]. We use the value $r = 1.6\,\mathrm{GeV}^{-1}$ from Ref. [14]. For the purpose of fitting the Δm distribution, we obtain $d\Gamma(\Delta m)/d\Delta m$ from Eqs. (1) and (2) through the substitution $m = m(D^0) + \Delta m$, where $m(D^0)$ is the nominal D^0 mass [15].

As in the CLEO analysis [8], we approximate the total D^{*+} decay width $\Gamma_{\mathrm{Total}}(m) \approx \Gamma_{D^*D\pi}(m)$, ignoring the electromagnetic contribution from $D^{*+} \to D^+\gamma$. This approximation has a negligible effect on the extracted values, as it appears only in the denominator of the RBW function.

To allow for differences between MC simulation and data, the root-mean-square deviation of each Gaussian component of the resolution function is allowed to scale in the fit process by the common factor $(1 + \epsilon)$. Events that contribute to the non-Gaussian component have a well-understood origin (π_s decay in flight), which is accurately reproduced by MC simulation. In the fit to data, the threshold function has a fixed shape and relative fraction, and is not convolved with the RBW. The relative contribution of the threshold function is small ($\lesssim 0.5\%$ of the signal), and the results from fits to validation signal-MC samples are unbiased without convolving this term. We fit the Δm distribution from the kinematic threshold to $\Delta m = 0.1665$ GeV using a binned maximum likelihood fit and an interval width of 50 keV.

In the initial fits to data, we observed a strong dependence of Δm_0 on the slow pion momentum. This dependence, which originates in the modeling of the magnetic field map and the material in the beam pipe and SVT, is not replicated in the simulation. Previous *BaBar* studies have observed this effect, for example the measurement of the Λ_c^+ mass [16]. In that analysis, the material model of the SVT was altered in an attempt to correct for the energy loss and the under-represented small-angle multiple scattering (due to nuclear Coulomb scattering). However, the momentum dependence could only be removed by adding a nonphysical amount of material to the SVT. The corrections used here avoid altering the underlying detector model and focus on adjusting track momenta following reconstruction. We use a sample of $K_S^0 \to \pi^+\pi^-$ events from $D^{*+} \to D^0\pi_s^+$ decays, where $D^0 \to K_S^0\pi^+\pi^-$, and require that the K_S^0 daughter pions satisfy the same tracking criteria as the π_s^+ candidates for the $D^0 \to K^-\pi^+$ and $D^0 \to K^-\pi^+\pi^-\pi^+$ signal modes. The K_S^0 decay vertex is required to lie inside the beam pipe and to be well separated from the D^0 vertex. These selection criteria yield an extremely clean K_S^0 sample (over 99.5% pure), which is used to determine fractional corrections to the overall magnetic field and to the energy losses in the beam pipe and, separately, in the SVT. We determine the best set of correction parameters by minimizing the difference between the $\pi^+\pi^-$ invariant mass and the current world average for the K^0 mass ($497.614 \pm 0.024\,\mathrm{MeV}$) [15] in 20 intervals of laboratory momentum in the range 0.0 to 2.0 GeV. The parameters increase the magnitude of the magnetic field by 4.5 Gauss and increase the energy loss in the beam pipe and SVT by 1.8% and 5.9%, respectively [11]. The momentum-dependence of Δm_0 in the preliminary results was mostly due to the slow pion. However, the correction is applied to all D^{*+} daughter tracks. All fits to data described in this analysis are performed using masses and Δm values calculated using corrected momenta. Simulated events do not require correction because the same field and material models used to propagate tracks are used for their reconstruction.

Figure 1 presents the results of the fits to data for both the $D^0 \to K^-\pi^+$ and $D^0 \to K^-\pi^+\pi^-\pi^+$ decay modes. The normalized residuals show good agreement between the data and our fits. Table I summarizes the results of the fits to data for both D^0 decay modes. The table also shows S/B at the peak and in the high Δm tail of each distribution.

We estimate systematic uncertainties related to a variety of sources. The data are divided into disjoint subsets corresponding to intervals of D^{*+} laboratory momentum, D^{*+} laboratory azimuthal angle ϕ, and reconstructed D^0 mass, in order to search for variations larger than those expected from statistical fluctuations. These are evaluated using a method similar to the PDG scale factor [11, 15]. The corrections to the momentum scale

TABLE I. Summary of the results from the fits to data for the $D^0 \to K^-\pi^+$ and $D^0 \to K^-\pi^+\pi^-\pi^+$ channels (statistical uncertainties only). S/B is the ratio of the convolved signal PDF to the background PDF at the given Δm and ν is the number of degrees of freedom.

Parameter	$D^0 \to K\pi$	$D^0 \to K\pi\pi\pi$
Number of signal events	$138\,539 \pm 109$	$174\,286 \pm 150$
$\Gamma\,[\text{keV}]$	83.5 ± 1.7	83.2 ± 1.5
scale factor, $(1+\epsilon)$	1.06 ± 0.01	1.08 ± 0.01
$\Delta m_0\,[\text{keV}]$	$145\,425.6 \pm 0.6$	$145\,426.6 \pm 0.5$
S/B at peak ($\Delta m = 0.14542\,[\text{GeV}]$)	2700	1130
S/B at tail ($\Delta m = 0.1554\,[\text{GeV}]$)	0.8	0.3
χ^2/ν	574/535	556/535

and dE/dx loss in detector material are varied to account for the uncertainty on the K^0_S mass. We estimate uncertainties related to our choice of the radius assumed in the Blatt-Weisskopf form factor, and vary the resolution shapes according to their uncertainties and correlations. We vary the end point used in the fit, which affects whether events are assigned to the signal or background component. This variation allows us to evaluate a systematic uncertainty associated with the background parametrization; within this systematic uncertainty, the residual plots shown in Fig. 1 are consistent with being entirely flat. Additionally, we vary the description of the background distribution near threshold. Finally, we assess systematic uncertainties associated with the interval width and possible biases observed in fits to MC validation samples with and without radiative effects. All these uncertainties are estimated independently for the $D^0 \to K^-\pi^+$ and $D^0 \to K^-\pi^+\pi^-\pi^+$ modes, as discussed in detail in Ref. [11] and summarized in Table II.

The largest systematic uncertainty arises from an observed sinusoidal dependence for Δm_0 on ϕ. Variations with the same signs and phases are seen for the reconstructed D^0 mass in both $D^0 \to K^-\pi^+$, $D^0 \to K^-\pi^+\pi^-\pi^+$, and for the K^0_S mass. An extensive investigation reveals that this dependence is most probably due to small sinusoidal variations in the magnetic field map used in track reconstruction [11]. The important aspect for this analysis is that the average value is unbiased by the variation in ϕ, which we verified using the reconstructed K^0_S mass value. The width does not display a ϕ dependence, but each mode is assigned a small uncertainty because some deviations from uniformity are observed. The lack of a systematic variation of Γ with respect to ϕ is notable because Δm_0 shows a clear dependence such that the results from the $D^0 \to K^-\pi^+$ and $D^0 \to K^-\pi^+\pi^-\pi^+$ samples are highly correlated and shift together. We fit the Δm_0 values with a sinusoidal function and take half of the amplitude as the estimate of the uncertainty.

The results for the two independent D^0 decay modes agree within their uncertainties. The dominant systematic uncertainty on the RBW pole position comes from the variation in ϕ (1.5-1.9 keV). For the decay mode $D^0 \to K^-\pi^+$ we find $\Gamma = (83.4 \pm 1.7 \pm 1.5)$ keV and $\Delta m_0 = (145\,425.6 \pm 0.6 \pm 1.8)$ keV, while for the decay mode $D^0 \to K^-\pi^+\pi^-\pi^+$ we find $\Gamma = (83.2 \pm 1.5 \pm 2.6)$ keV and $\Delta m_0 = (145\,426.6 \pm 0.5 \pm 2.0)$ keV. Accounting for correlations, we obtain the combined measurement values $\Gamma = (83.3 \pm 1.3 \pm 1.4)$ keV and $\Delta m_0 = (145\,425.8 \pm 0.5 \pm 1.8)$ keV.

Using the relationship between the width and the coupling constant [11], we can determine the experimental value of $g_{D^{*+}D^0\pi^+}$. Using Γ and the masses from Ref. [15] we determine the experimental coupling $g^{\text{exp}}_{D^{*+}D^0\pi^+} = 16.92 \pm 0.13 \pm 0.14$, where we have ignored the electromagnetic contribution from $D^{*+} \to D^+\gamma$. The universal coupling is directly related to $g_{D^*D\pi}$ by $\hat{g} = g_{D^{*+}D^0\pi^+} f_\pi / \left(2\sqrt{m_{D^0} m_{D^{*+}}}\right)$. This parametrization is different from that used by CLEO [8]; it is chosen to match a common convention in the context of chiral perturbation theory, as in Refs. [4, 17]. With this relation and $f_\pi = 130.41\,\text{MeV}$, we find $\hat{g}^{\text{exp}} = 0.570 \pm 0.004 \pm 0.005$.

Di Pierro and Eichten [18] present results in terms of R, the ratio of the width of a given state to the universal coupling constant. At the time of their publication, $\hat{g} = 0.82 \pm 0.09$ was consistent with the values from all of the modes in Ref. [18]. In 2010, *BABAR* published much more precise mass and width results for the $D_1(2460)^0$ and $D^*_2(2460)^0$ mesons [19]. Using these values, our measurement of Γ, and the ratios from Ref. [18], we calculate new values for the coupling constant $\hat{g}$. Table III shows the updated results. We estimate the uncertainty on $\hat{g}$ assuming $\sigma_\Gamma \ll \Gamma$. The updated widths reveal significant differences among the extracted values of $\hat{g}$. The order of magnitude increase in precision of the D^{*+} width measurement compared to previous studies confirms the observed inconsistency between the measured D^{*+} width and the chiral quark model calculation by Di Pierro and Eichten [18].

We are grateful for the excellent luminosity and machine conditions provided by our PEP-II colleagues, and for the substantial dedicated effort from the computing organizations that support *BABAR*. The collaborating institutions wish to thank SLAC for its support and kind hospitality. This work is supported by DOE and NSF (USA), NSERC (Canada), CEA and CNRS-IN2P3 (France), BMBF and DFG (Germany), INFN (Italy), FOM (The Netherlands), NFR (Norway), MES (Russia), MINECO (Spain), STFC (United Kingdom). Individuals have received support from the Marie Curie EIF (European Union) and the A. P. Sloan Foundation (USA).

TABLE II. Summary of systematic uncertainties with correlation ρ between the $D^0 \to K^-\pi^+$ and $D^0 \to K^-\pi^+\pi^-\pi^+$ modes. The $K^-\pi^+$ and $K^-\pi^+\pi^-\pi^+$ invariant masses are denoted by $m\left(D^0_{\rm reco}\right)$.

Source	$\sigma_{sys}(\Gamma)$ [keV]		ρ	$\sigma_{sys}(\Delta m_0)$ [keV]		ρ
	$K\pi$	$K\pi\pi\pi$		$K\pi$	$K\pi\pi\pi$	
Disjoint D^{*+} momentum bin variation	0.88	0.98	0.47	0.24	0.20	0.28
Disjoint $m\left(D^0_{\rm reco}\right)$ bin variation	0.00	1.53	0.56	0.04	0.00	0.22
Disjoint azimuthal variation	0.62	0.92	-0.04	1.65	1.81	0.84
Magnetic field and material model	0.29	0.18	0.98	0.75	0.81	0.99
Blatt-Weisskopf radius	0.04	0.04	0.99	0.00	0.00	1.00
Variation of resolution shape parameters	0.41	0.37	0.00	0.17	0.16	0.00
Δm fit range	0.83	0.38	-0.42	0.08	0.04	0.35
Background shape near threshold	0.10	0.33	1.00	0.00	0.00	0.00
Interval width for fit	0.00	0.05	0.99	0.00	0.00	0.00
Bias from validation	0.00	1.50	0.00	0.00	0.00	0.00
Radiative effects	0.25	0.11	0.00	0.00	0.00	0.00
Total	1.5	2.6		1.8	2.0	

TABLE III. Updated coupling constant values using the latest width measurements. Ratios are taken from Ref. [18].

State	Width (Γ)	$R = \Gamma/\hat{g}^2$ (model)	$\hat{g}$
$D^*(2010)^+$	$83.3 \pm 1.3 \pm 1.4\,\mathrm{keV}$	$143\,\mathrm{keV}$	0.76 ± 0.01
$D_1(2420)^0$	$31.4 \pm 0.5 \pm 1.3\,\mathrm{MeV}$	$16\,\mathrm{MeV}$	1.40 ± 0.03
$D_2^*(2460)^0$	$50.5 \pm 0.6 \pm 0.7\,\mathrm{MeV}$	$38\,\mathrm{MeV}$	1.15 ± 0.01

The University of Cincinnati is gratefully acknowledged for its support of this research through a WISE (Women in Science and Engineering) fellowship to C. Fabby.

* Now at the University of Tabuk, Tabuk 71491, Saudi Arabia
† Also with Università di Perugia, Dipartimento di Fisica, Perugia, Italy
‡ Now at the University of Huddersfield, Huddersfield HD1 3DH, UK
§ Deceased
¶ Now at University of South Alabama, Mobile, Alabama 36688, USA
** Also with Università di Sassari, Sassari, Italy
†† Now at Universidad Técnica Federico Santa Maria, Valparaiso, Chile 2390123

[1] D. Becirevic and A. L. Yaouanc, JHEP **03**, 021 (1999).
[2] P. Singer, Acta Phys. Pol. B **30**, 3849 (1999).
[3] D. Guetta and P. Singer, Nucl. Phys. Proc. Suppl. **93**, 134 (2001).
[4] B. El-Bennich, M. A. Ivanov, and C. D. Roberts, Phys. Rev. C **83**, 025205 (2011).
[5] G. Burdman *et al.*, Phys. Rev. D **49**, 2331 (1994).
[6] C. Arnesen *et al.*, Phys. Rev. Lett. **95**, 071802 (2005).
[7] J. Bailey *et al.*, Phys. Rev. D **79**, 054507 (2009).
[8] A. Anastassov *et al.* (CLEO Collaboration), Phys. Rev. D **65**, 032003 (2002).
[9] S. Agostinelli *et al.* (Geant4 Collaboration), Nucl. Instr. Methods Phys. Res., Sect. A **506**, 250 (2003).
[10] B. Aubert *et al.* (*BABAR* Collaboration), Nucl. Instr. Methods Phys. Res., Sect. A **479**, 1 (2002).
[11] J. P. Lees *et al.* (*BABAR* Collaboration), Submitted to Phys. Rev. D (2013), arXiv:1304.5009 [hep-ex].
[12] J. M. Blatt and V. F. Weisskopf, *Theoretical Nuclear Physics* (John Wiley & Sons, New York, 1952).
[13] F. von Hippel and C. Quigg, Phys. Rev. D **5**, 624 (1972).
[14] A. J. Schwartz (for the E791 Collaboration), arXiv:hep-ex/0212057. Contribution to 5th International Conference
[15] J. Beringer *et al.* (Particle Data Group), Phys. Rev. D **86**, 010001 (2012).
[16] B. Aubert *et al.* (*BABAR* Collaboration), Phys. Rev. D **72**, 052006 (2005).
[17] A. Abada *et al.*, Phys. Rev. D **66**, 074504 (2002).
[18] M. Di Pierro and E. Eichten, Phys. Rev. D **64**, 114004 (2001).
[19] P. del Amo Sanchez *et al.* (*BABAR* Collaboration), Phys. Rev. D **82**, 111101(R) (2010).